



CrossMark  
click for updates

Cite this: *RSC Adv.*, 2016, 6, 90018

Received 1st June 2016  
Accepted 5th September 2016

DOI: 10.1039/c6ra14248f

www.rsc.org/advances

# Preparation of Schiff base decorated graphene oxide and its application in TPU with enhanced thermal stability

Yulu Zhu,<sup>a</sup> Yongqian Shi,<sup>a</sup> Zhengqi Huang,<sup>a</sup> Lijin Duan,<sup>a</sup> Yuan Hu<sup>\*a</sup> and Xinlong Gong<sup>\*ab</sup>

A facile *in situ* method of synthesis and immobilization of a copper(salen) complex onto graphene oxide (GO) support has been developed. Thermoplastic polyurethane (TPU) nanocomposites were manufactured using a master batch-melt compounding approach, in which the nanohybrid material was added into a TPU matrix. Observed enhancements in the thermal stability and flame retardancy were ascribed to graphene oxide nanosheets functioning as physical barriers, as well as to the catalysis of the decomposition reaction by both copper chelates and Schiff bases to obtain increased char residues.

## 1. Introduction

Hugo Schiff first condensed an aldehyde with an amine to generate what is now known as a Schiff base in 1864.<sup>1</sup> Rich structural diversification, application and proliferation of Schiff bases have occurred since that time. Either alone or in metal-chelated form, Schiff bases are widely applied in drug discovery,<sup>2</sup> nonlinear optical materials,<sup>3</sup> electrochemical cells, corrosion inhibitors,<sup>4</sup> molecular sensors/photonic devices, magnetic materials,<sup>5</sup> and flame retardants.<sup>6,7</sup> The salen ligand is a member of the Schiff base family. Fontaine *et al.*<sup>8,9</sup> reported salen and its metal chelates that were halogen free, non-phosphorus containing, and based on a relatively simple organic framework, which resulted in improved thermal stability and flame retardant properties of thermoplastic polyurethane elastomer (TPU). The standard Schiff base motif involves nitrogen as the basic element. They offer two advantages as raw materials for producing flame retardants.<sup>10</sup> First, a flexible synthetic approach can be developed for preparation of structurally diverse Schiff bases with various substituents. Second, the thermal and nonflammable properties of the Schiff

base moieties can be conferred to their derivatives.<sup>11</sup> However, owing to their “soft” molecular network, scarcely any work has been performed surrounding their use for high-temperature thermal protective applications, such as flame retardants or ablative materials, both of which are vital components of contemporary engineering materials.<sup>7</sup> Immobilization of metal complexes on solid supports is an efficient strategy to enhance their catalytic performance<sup>12,13</sup> and is also expected to remedy the drawback of the “soft” molecular network. Herein, we report immobilization of metal-Schiff base complex copper(salen) onto solid graphene oxide supports.

In recent years, polymer nanocomposites have become an alternative solution to reducing the flammability of polymers *via* an additive approach.<sup>14–16</sup> Carbon nanoadditives, including graphite oxide (GO)<sup>17,18</sup> and carbon nanotubes,<sup>19,20</sup> have been extensively explored because of their ability to increase both the mechanical strength and electronic conductivity of the native polymer. Of these nanoadditives, graphene oxide (GO), which shares the same framework as graphene, but with heterogeneous chemical and electronic structures,<sup>21</sup> a unique two-dimensional structure and outstanding performance, along with the fact that it can be processed in a solution, has attracted great interest and wide study. It is widely reported that GO can be effective as a flame retardant.<sup>22–24</sup> Higginbotham<sup>25</sup> *et al.* studied the effect of GO addition on the mechanical strength and flammability of polymers, including polycarbonate, acrylonitrile butadiene styrene, and high-impact polystyrene, demonstrating reduced flammability of the materials as the content of GO increased. The total heat release (THR) and peak heat release rate (pHRR) decreased, and the char yield increased according to the same trend.

It is well known that GO nanosheets produced from graphite using Hummers' method are endowed with numerous oxygen containing functional groups such as  $-\text{COOH}$ ,  $-\text{C}=\text{O}$ , and  $-\text{OH}$ . 3-Amino-propyltriethoxysilane (APTS) is used to covalently modify the surface of GO. APTS is a frequently used silane coupling agent with an amino group,<sup>26</sup> which effect silylation of the surface hydroxyl groups of GO.

<sup>a</sup>State Key Laboratory of Fire Science, University of Science and Technology of China, 96 Jinzhai Road, Hefei, Anhui 230026, P. R. China. E-mail: yuanhu@ustc.edu.cn; gongxl@ustc.edu.cn; Fax: +86-551-3601664; Tel: +86-551-3601664

<sup>b</sup>CAS Key Laboratory of Mechanical Behavior and Design of Materials, Department of Modern Mechanics, University of Science and Technology of China, China

TPU is a typical thermoplastic elastomer, possessing the mechanical properties of vulcanized rubber and the processability of thermoplastic polymers; hence, it is considered as one of the most versatile polymers. It is widely applied in various areas such as adhesives, sealants, coatings, fibers, injection molded components, thermoplastic parts, industrial cables, energy exploration, automotive and transportation.<sup>27</sup> However, several fatal drawbacks greatly limit its further application, such as high flammability and evolution of large amounts of smoke and combustible volatiles during combustion. It is expected that combination of Schiff bases and GO can contribute to improvements in thermal stability and flame retardancy of TPU.

In this study, synthesis and immobilization of a Cu(salen) complex onto GO nanosheets using a facile method has been introduced. GO was covalently modified with aminosilane to support the salen ligands, and subsequently condensed with copper nitrate to simultaneously form metal chelates and to immobilize the pre-formed Cu(salen) complex onto its surface (sample name: Cu(salen)-f-GO). Finally, the functionalized GO nanosheets were added into TPU and tested for reducing its fire hazards. The combination of the lamellar barrier effect of GO nanosheets and the catalytic effect of both copper chelates and Schiff bases will lead to an improvement in the thermal stability and fire resistance properties of the polymer nanocomposites.

The aim of our present study is to reduce fire hazards and improve the thermal stability of TPU using Cu(salen)-f-GO nanosheets. The structure and morphology of the as-prepared Cu(salen)-f-GO nanosheets were characterized by X-ray powder diffraction (XRD), transmission electron microscopy (TEM) and X-ray photoelectron spectrometry (XPS). In addition, the thermal stability and flame retardancy of TPU nanocomposites were evaluated by thermogravimetric analysis (TGA) and cone calorimetry, respectively. The mechanism for the reduction in fire hazards of the TPU nanocomposites was also discussed.

## 2. Experimental section

### 2.1. Raw materials

TPU (85E85) was obtained from Baoding Bangtai Chemical Industry Co., Ltd. (Baoding, China), copper nitrate trihydrate ( $\text{Cu}(\text{NO}_3)_2 \cdot 3\text{H}_2\text{O}$ ), *N,N*-dimethylformamide (DMF), methanol, salicylaldehyde, glacial acetic acid, APTS and anhydrous ethanol were purchased from Sinopharm Chemical Reagent Co., Ltd. (Shanghai, China). All the reagents were used as received without further purification.

### 2.2. Preparation of GO and APTS-f-GO

GO was prepared using the Hummers' method according to a previous report.<sup>26</sup> 0.25 g of GO was dispersed in 60 mL of anhydrous ethanol in a 250 mL three-necked round-bottom flask, followed by ultrasonication assisted stirring for 30 min. Around 30 mL of ethanol solution containing 0.443 g of APTS was added dropwise into the slurry at ambient temperature. The mixture was kept under nitrogen at 78 °C with agitation and refluxed overnight. APTS-f-GO was finally obtained by filtering

and repeatedly washing with acetone, followed by drying in a vacuum oven at 50 °C overnight. The product, APTS-f-GO, was dark in color.

### 2.3. Synthesis of Cu(salen)-f-GO

The resulting APTS-f-GO was dispersed in 60 mL of absolute ethanol. 3.0 mmol of salicylaldehyde was added into the suspension with drops of glacial acetic acid as an accelerator. After refluxing for 5 h and cooling, the crystals were filtered and washed with methanol several times. Finally, the solid, together with 2.0 mmol of  $\text{Cu}(\text{NO}_3)_2 \cdot 3\text{H}_2\text{O}$ , was dispersed in methanol and agitated for 12 h at ambient temperature. The obtained mixture was filtered, washed, and dried at 50 °C. The schematic to illustrate the preparation of Cu(salen)-f-GO is presented in Fig. 1.

### 2.4. Preparation of TPU nanocomposites

A TPU solution was obtained by dissolving TPU in DMF at 80 °C. The desired concentration of Cu(salen)-f-GO nanosheets was dispersed in ethanol under sonication for 20 min and was then added to the TPU solution. The mixture was further treated under sonication-assisted agitation for 1 h. The hot mixture was poured into distilled water to precipitate the TPU/Cu(salen)-f-GO master batch. This obtained master batch was separated by filtration and dried overnight. Finally, the masterbatch was mixed with pure TPU to prepare TPU/Cu(salen)-f-GO nanocomposites containing 0.5 wt% Cu(salen)-f-GO nanohybrids (named TPU0.5) through a melt blending approach. The same procedure was performed to fabricate products containing 1.0 wt% Cu(salen)-f-GO (named TPU1.0) and 2.0 wt% Cu(salen)-f-GO (named TPU2.0).

### 2.5. Characterization

XRD patterns were measured by a Japan Rigaku Dmax X-ray diffractometer equipped with graphite mono-chromatic high-intensity Cu K $\alpha$  radiation ( $\lambda = 1.54178 \text{ \AA}$ ). Fourier transform infrared (FTIR) spectrum analyses were operated on samples pelletized with KBr powders in the range of 4000–400  $\text{cm}^{-1}$  using an IR Fourier transform spectrophotometer (Nicolet,

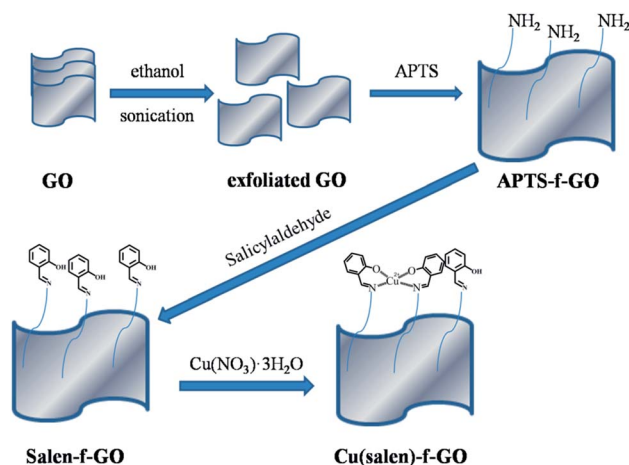


Fig. 1 Illustration for the synthetic methodology of Cu(salen)-f-GO.

ZOSX). TEM was performed by a JEOL2010 instrument with an acceleration voltage of 200 kV. The dispersion of GO, APTS-f-GO and Cu(salen)-f-GO in ethanol was treated with sonication, and then dripped onto copper grids before observation. Scanning electron microscopy (SEM) images were obtained with a scanning electron microscope AMRAY1000B at an accelerating voltage of 20 kV. XPS spectra were obtained using a Kratos Axis Ultra DLD spectrometer employing a mono-chromatic Al K $\alpha$  X-ray source ( $h\nu = 1486.6$  eV). TGA of TPU and its nanocomposites was performed using a Q5000 device. Thermal analysis was conducted in the range from room temperature to 800 °C with a heating rate of 20 °C min<sup>-1</sup> under a helium atmosphere.

### 3. Results and discussion

#### 3.1. The structure and morphology of GO and Cu(salen)-f-GO

All the samples were investigated by XRD to confirm their phases, as shown in Fig. 2. The characteristic diffraction peak of GO is located at  $2\theta = 10.3^\circ$ , corresponding to the (002) reflection and is attributed to an inter-planar spacing of 0.84 nm. There is a weak peak located at  $2\theta = 42^\circ$  corresponding to the (100) reflection. Upon silane covalent functionalization with APTS, the diffraction peak shifts to  $6.7^\circ$ , indicating that interlayer spacing was significantly enlarged. This shift confirmed that APTS was successfully inserted into GO *via* hydrolytic condensation.<sup>28</sup> The enlarged intra-gallery space of GO is attributed to the silane covalent functionalization.<sup>29</sup>

FTIR spectra of pristine GO, APTS modified GO (APTS-f-GO), and Cu(salen)-f-GO are shown in Fig. 2a. Compared to unmodified GO, APTS-f-GO shows additional strong bands at 1120 and 1038 cm<sup>-1</sup>, which are attributed to characteristic absorption of Si-O bonds acquired during the silylation process. The new bands appearing at 2928 and 2860 cm<sup>-1</sup> correspond to stretching vibrations of the C-H bond, and the bands located at around 3220 and 1570 cm<sup>-1</sup> are assigned to the vibrations of the N-H bond, further verifying that the amino-silane chains were successfully introduced. After condensation with salicylaldehyde, the N-H absorbance range shows a significant decrease, while an additional sharp band near

1625 cm<sup>-1</sup> arises that is associated with the stretching vibrations of C=N. The absorption from the benzene rings of salicylaldehyde presents peaks in the range of 1400–1600 cm<sup>-1</sup>. It can be noted that free C=N vibrations are generally located at around 1640 cm<sup>-1</sup>, and therefore the shift towards lower values of approximately 15 cm<sup>-1</sup> in Cu(salen)-f-GO could be ascribed to coordination interactions with the copper ions. These results demonstrate that the salen ligands are bound to copper and anchored onto the GO surface.

The surface electronic states of the samples and the interaction between GO and APTS were assessed by XPS. As shown in Fig. 3a, Si and N signals appear after the silylation modification. In addition, a Cu signal is detected for Cu(salen)-f-GO. Furthermore, APTS-f-GO exhibits an obvious decrease of around 286.5 eV in the C-O-C and C-OH band as compared with the C 1s spectrum of unmodified GO. The Cu 2p XPS spectrum of Cu(salen)-f-GO shows two typical bands at 933.9 and 953.8 eV, which correspond to the bonding energy of copper(II). Moreover, a Cu 2p<sub>3/2</sub> satellite peak at 943.0 eV occurs, demonstrating the coordination interaction between the salen ligand and the copper center.<sup>30–32</sup>

TEM measurements were performed to investigate the morphology and microstructure of the as-synthesized samples. Fig. 4a presents a representative TEM image of unmodified GO nanosheets, showing that they are ripped and paper-like with size of *ca.* 1  $\mu\text{m}$ . However, after the silylation modification, the color of the nanosheets appears a little deeper, although the ripped and paper-like morphology was maintained. This observation reflects that the thickness of the nanosheets has increased, which is consistent with previous literature reports.<sup>33</sup> Fig. 4c and d present SEM images of APTS-f-GO and Cu(salen)-f-GO, showing that these nanosheets are wrinkled and stacked.

#### 3.2 Thermal behavior of TPU and its nanocomposites

TGA is an effective technique for estimating thermal stability of polymeric materials. The TG and DTG curves of TPU and its nanocomposites are presented in Fig. 5, and the corresponding data are recorded in Table 1. The temperatures at which 10% mass loss, 50% mass loss and maximum mass loss occur are defined as the measurement of initial degradation temperature

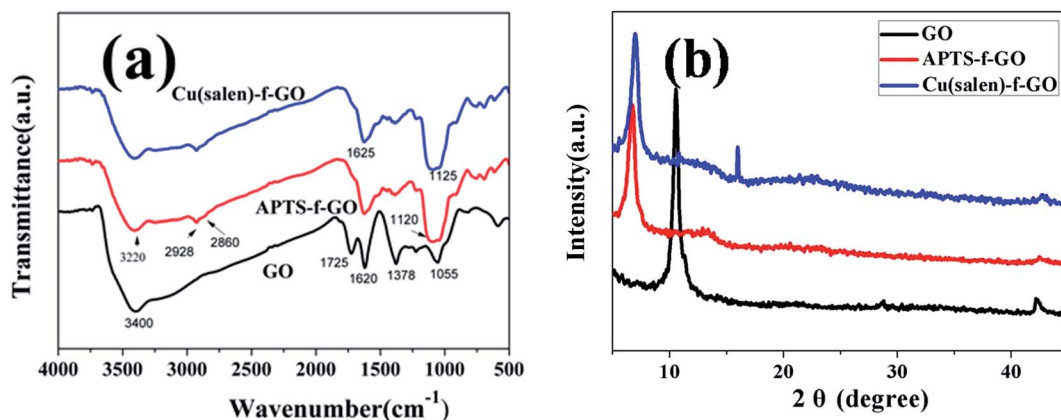


Fig. 2 FTIR spectra (a) and XRD patterns (b) of GO, APTS-f-GO and Cu(salen)-f-GO.

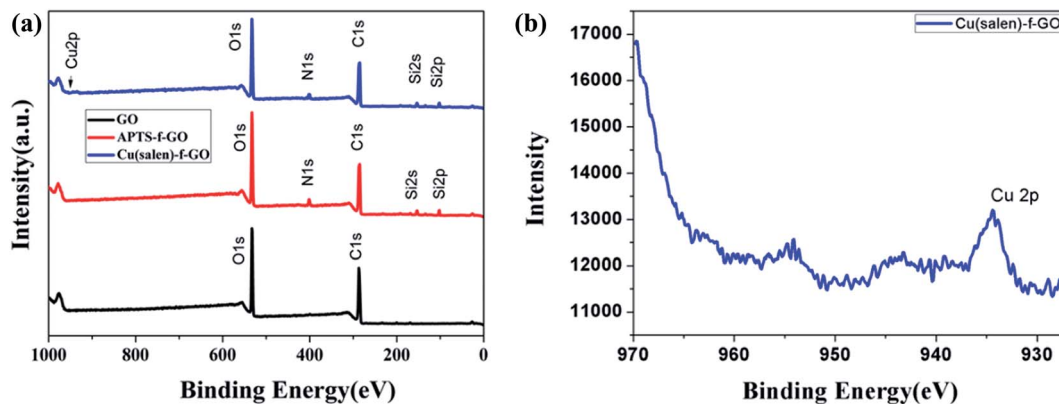


Fig. 3 Full range XPS spectra of GO, APTS-f-GO, and Cu(salen)-f-GO (a), Cu 2p XPS spectrum of Cu(salen)-f-GO (b).

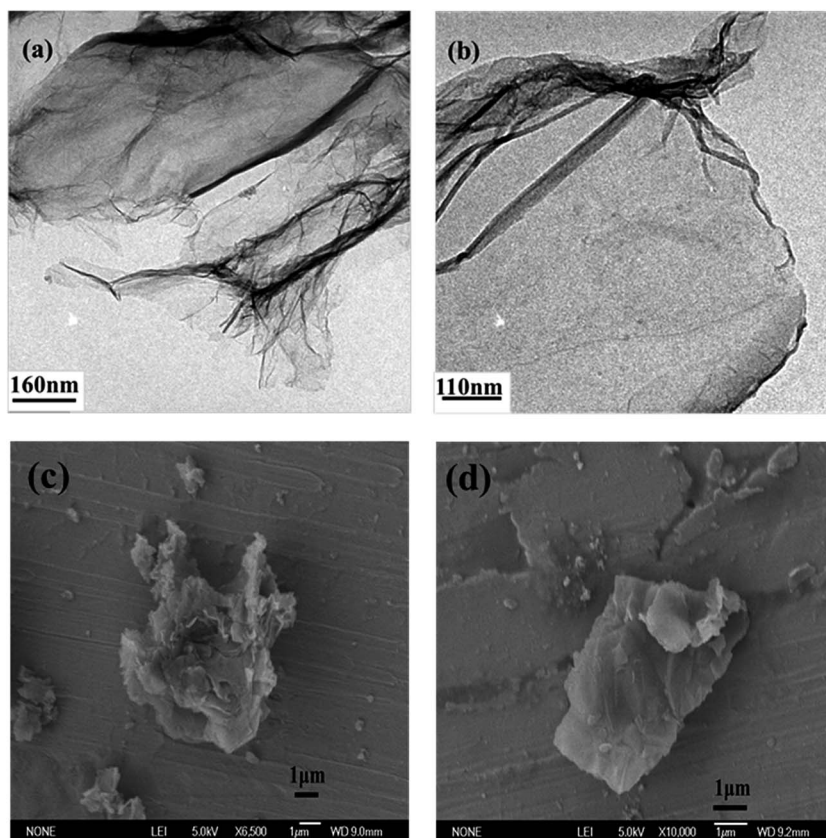


Fig. 4 TEM images of APTS-f-GO (a) and Cu(salen)-f-GO (b); SEM images of APTS-f-GO (c) and Cu(salen)-f-GO (d).

( $T_{10}$ ), half degradation temperature ( $T_{50}$ ), and maximum degradation temperature ( $T_{max}$ ), respectively. As can be seen from Fig. 5, all the nanocomposites exhibit similar thermal degradation behavior when compared to pure TPU. However, the nanocomposites have a residual yield several times higher than that of pristine TPU. Furthermore, the degradation temperature of the nanocomposites increased gradually with increased loading. For instance, the  $T_{max}$  of TPU2.0 is increased by 32.7 °C over that of TPU, indicating an improved thermal stability of the nanocomposites. In addition, the char residue of Cu(salen)-f-GO at 700 °C is significantly increased due to the catalytic

carbonization of Cu(salen) and the lamellar barrier effect of GO nanosheets.<sup>34,35</sup> The improved char yield provides a protective shield to mass and heat transfer, thereby reducing the heat release rate during combustion and remarkably improving the thermal stability, as evidenced by the increased  $T_{max}$ .

### 3.3. Flame retardancy evaluation of TPU and its nanocomposites

Fig. 6 shows the values of HRR collected from the cone calorimeter. The heat release rate, particularly for the peak heat

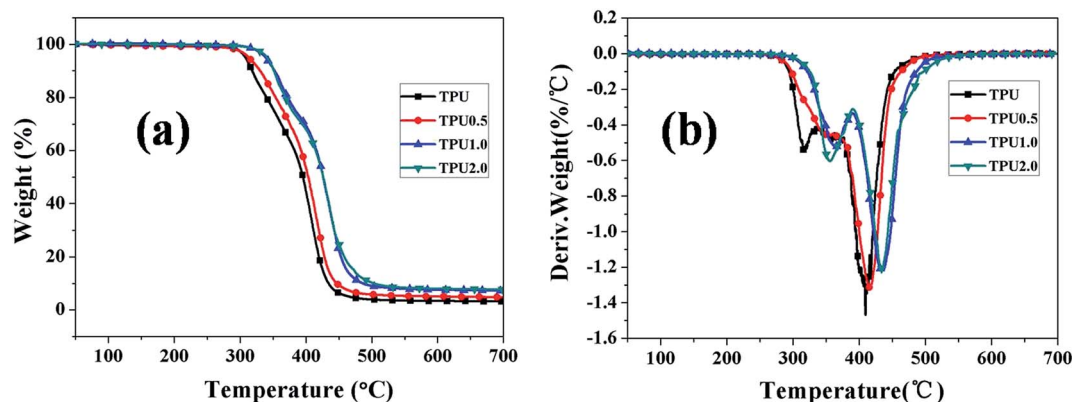


Fig. 5 TG (a) and DTG (b) curves of TPU and its nanocomposites.

Table 1 Summary of TGA data of TPU and its nanocomposites

Sample no.	$T_{10}$	$T_{max}$	$T_{50}$	Char residues at 700 °C (wt%, measured)
TPU	318.2	409.3	395.4	3.1
TPU0.5	330.3	420.6	403.5	4.5
TPU1.0	352.2	436.9	426.0	7.0
TPU2.0	351.2	442.0	426.2	7.4

release rate (pHRR) value, is usually considered to be a key parameter when measuring fire safety. This is because pHRR represents the point in a fire where heat is likely to propagate further or ignite adjacent objects; thus, a reduction in pHRR is highly desirable and of great significance.<sup>36</sup> It is observed that TPU0.5, TPU1.0 and TPU2.0 exhibit a decline in pHRR. The largest reduction is obtained for TPU2.0, *i.e.*, a decrease of 14% was observed compared to neat TPU. This result can be attributed to GO nanosheets having a physical barrier effect, which slows down the heat release and can effectively delay transfer of heat, oxygen and volatile gases. However, the physical barrier

effect is not enough to reduce the pHRR substantially at lower loadings. Catalytic charring of Cu(salen) leads to the formation of additional char yield, which provides a further protective shield for mass and heat transfer and thus slows down the thermal decomposition rate of the material.

## 4. Conclusions

In summary, GO nanosheets were functionalized with Cu(salen) *via* a facile method, and then incorporated into TPU to fabricate polymer nanocomposites. TGA results demonstrated that the  $T_{10}$  and char yield were markedly improved for TPU/Cu(salen)-f-GO composites. In particular, a decrease of 14% in pHRR was obtained for TPU2.0. A possible mechanism for the reduced fire hazards of TPU/Cu(salen)-f-GO systems was proposed. On one hand, GO provided a physical barrier effect. On the other hand, Cu(salen) moieties led to increased char residues, which provided further protection and increased the thermal stability and flame retardancy.

## Acknowledgements

This study was financially supported by the National Basic Research Program of China (973 Program) (No. 2012CB719701), the National Natural Science Foundation of China (No. 21374111, 21411140231), and the Fundamental Research Funds for the Central Universities (No. WK2320000032).

## Notes and references

- 1 H. Schiff, *Ann. Suppl.*, 1864, 3, 343.
- 2 O. Ramstrom and J. M. Lehn, *Nat. Rev. Drug Discovery*, 2002, 1, 26–36.
- 3 P. G. Lacroix, *Eur. J. Inorg. Chem.*, 2001, 339–348.
- 4 M. M. Antonijevic and M. B. Petrovic, *Int. J. Electrochem. Sci.*, 2008, 3, 1–28.
- 5 M. Andruh, *Chem. Commun.*, 2011, 47, 3025–3042.
- 6 A. M. Atta, N. O. Shaker and N. E. Maysour, *Prog. Org. Coat.*, 2006, 56, 100–110.

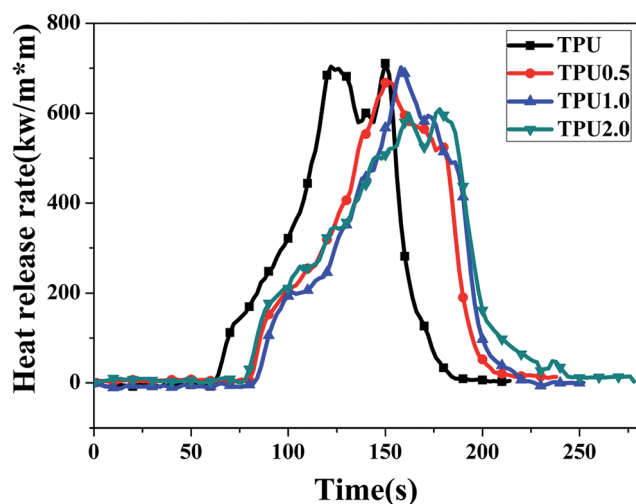


Fig. 6 HRR curves of TPU and its nanocomposites.

- 7 A. D. Naik, G. Fontaine, S. Bellayer and S. Bourbigot, *ACS Appl. Mater. Interfaces*, 2015, **7**, 21208–21217.
- 8 G. Fontaine, T. Turf and S. Bourbigot, *ACS Symp. Ser.*, 2009, 329–340.
- 9 A. D. Naik, G. Fontaine, S. Bellayer and S. Bourbigot, *RSC Adv.*, 2015, **5**, 48224–48235.
- 10 Y. Xiong, Z. Jiang, Y. Xie, X. Zhang and W. Xu, *J. Appl. Polym. Sci.*, 2013, **127**, 4352–4358.
- 11 Y. Liu, Y. Zhang, Z. Cao and Z. Fang, *Fire Saf. J.*, 2013, **61**, 185–192.
- 12 R. Kitaura, G. Onoyama, H. Sakamoto, R. Matsuda, S. I. Noro and S. Kitagawa, *Angew. Chem., Int. Ed.*, 2004, **116**, 2738–2741.
- 13 Z. Li, S. Wu, H. Ding, D. Zheng, J. Hu, X. Wang, Q. Huo, J. Guan and Q. Kan, *New J. Chem.*, 2013, **37**, 1561–1568.
- 14 J. W. Gilman, T. Kashiwagi and J. D. Lichtenhan, *SAMPE J.*, 1997, **33**, 40–46.
- 15 S. Bourbigot and S. Duquesne, *J. Mater. Chem.*, 2007, **17**, 2283–2300.
- 16 I. D. Carja, D. Serbezeanu, T. Vlad-Bubulac, C. Hamciuc, A. Coroaba, G. Lisa, C. G. Lopez, M. F. Soriano, V. F. Perez and M. D. R. Sanchez, *J. Mater. Chem. A*, 2014, **2**, 16230–16241.
- 17 D. K. Chattopadhyay and D. C. Webster, *Prog. Polym. Sci.*, 2009, **34**, 1068–1133.
- 18 Y. Q. Guo, C. L. Bao, L. Song, B. H. Yuan and Y. Hu, *Ind. Eng. Chem. Res.*, 2011, **50**, 7772–7783.
- 19 T. Kashiwagi, F. M. Du, J. F. Douglas, K. I. Winey, R. H. Harris and J. R. Shields, *Nat. Mater.*, 2005, **4**, 928–933.
- 20 L. Liu and J. C. Grunlan, *Adv. Funct. Mater.*, 2007, **17**, 2343–2348.
- 21 K. P. Loh, Q. Bao, G. Eda and M. Chhowalla, *Nat. Chem.*, 2010, **2**, 1015–1024.
- 22 S.-D. Jiang, Z.-M. Bai, G. Tang, L. Song, A. A. Stec, T. R. Hull, J. Zhan and Y. Hu, *J. Mater. Chem. A*, 2014, **2**, 17341–17351.
- 23 B. H. Yuan, C. L. Bao, L. Song, N. N. Hong, K. M. Liew and Y. Hu, *Chem. Eng. J.*, 2014, **237**, 411–420.
- 24 C. L. Bao, Y. Q. Guo, L. Song, Y. C. Kan, X. D. Qian and Y. Hu, *J. Mater. Chem.*, 2011, **21**, 13290–13298.
- 25 A. L. Higginbotham, J. R. Lomeda, A. B. Morgan and J. M. Tour, *ACS Appl. Mater. Interfaces*, 2009, **1**, 2256–2261.
- 26 W. S. Hummers Jr and R. E. Offeman, *J. Am. Chem. Soc.*, 1958, **80**, 1339.
- 27 Y. Shi, B. Yu, K. Zhou, R. K. Yuen, Z. Gui, Y. Hu and S. Jiang, *J. Hazard. Mater.*, 2015, **293**, 87–96.
- 28 M. Zhang, H. Yan, X. Yang and C. Liu, *RSC Adv.*, 2014, **4**, 45930–45938.
- 29 C. Liu, H. Yan, Z. Chen, L. Yuan and Q. Lv, *RSC Adv.*, 2015, **5**, 46632–46639.
- 30 Z. Zude, Z. Xiong, Z. Tao, Y. Huaming and L. Qingliang, *J. Mol. Struct.*, 1999, **478**, 23–27.
- 31 M. Orio, O. Jarjays, H. Kanso, C. Philouze, F. Neese and F. Thomas, *Angew. Chem.*, 2010, **122**, 5109–5112.
- 32 B. Fan, H. Li, W. Fan, C. Jin and R. Li, *Appl. Catal., A*, 2008, **340**, 67–75.
- 33 H. Yang, F. Li, C. Shan, D. Han, Q. Zhang, L. Niu and A. Ivaska, *J. Mater. Chem.*, 2009, **19**, 4632–4638.
- 34 D.-Y. Wang, Y. Liu, Y.-Z. Wang, C. P. Artiles, T. R. Hull and D. Price, *Polym. Degrad. Stab.*, 2007, **92**, 1592–1598.
- 35 Y. Shi, X. Qian, K. Zhou, Q. Tang, S. Jiang, B. Wang, B. Wang, B. Yu, Y. Hu and R. K. Yuen, *Ind. Eng. Chem. Res.*, 2013, **52**, 13654–13660.
- 36 H. Pan, Y. Lu, L. Song, X. Zhang and Y. Hu, *Compos. Sci. Technol.*, 2016, **129**, 116–122.